Supporting Information

Growth of MgO doped near stoichiometric $LiNbO_3$ single crystal by hanging crucible Czochralski method with ship lockage type powder feeding system assisted by numerical simulation†

Tao Yan,[ac] Yanhua Leng,[‡a] Yonggui Yu,[b] Dehui Sun,[a] Jie Zhan,[a] Wan Hairul Anuar Kamaruddin,[d] Xiaoyong Qin,[b] Xuxia Shi,[b] Liuwen Chang,[c] Mitch M. C. Chou,[c] Jiyang Wang*[a] and Hong Liu*[a]

<u>Hanging crucible Czochralski apparatus and feeding system</u>

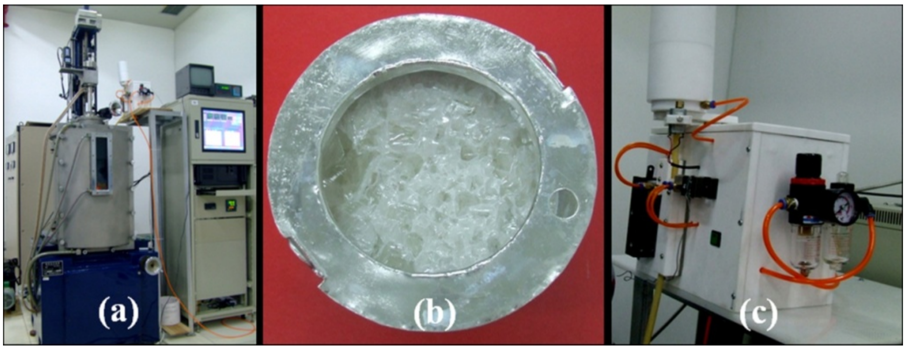

Fig. S1 Photographs of (a) Growth apparatus, (b) HCCZ crucible system, and (c) ship lockage type powder feeding system.

[a]*State Key Laboratory of Crystal Materials, Shandong University, Jinan 250100, China. E-mail: hongliu@sdu.edu.cn (Hong Liu), jywang@sdu.edu.cn (Jiyang Wang)*
[b]*CETC Deqing Huaying Electronics Co., Ltd, Deqing 313200, China.*
[c]*Department of Materials and Optoelectronic Science, National Sun Yat-sen University, Kaohsiung 80424, Taiwan.*
[d.]*Department of Physics, Faculty of Science, Universiti Teknologi Malaysia, 81310 UTM Skudai, Johor, Malaysia.*
† Electronic supplementary information (ESI) available. See DOI: 10.1039/b000000x/
‡ Co-first author.

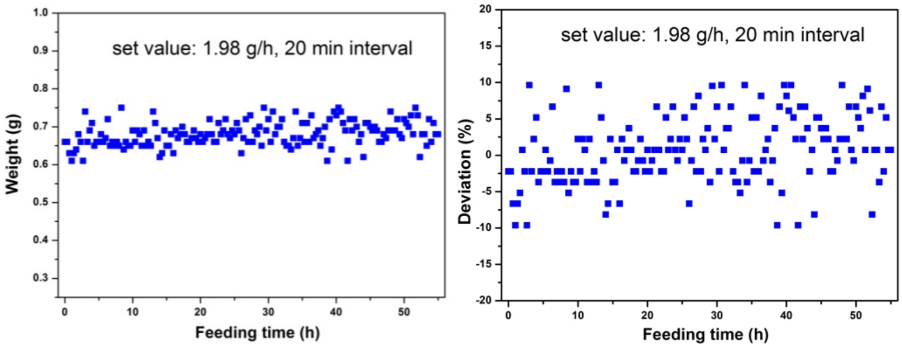

(a) (b)

Fig. S2 (a) Weight of feeding powders and (b) the corresponding deviation from a set value as a function of feeding time.

Numerical simulation for SLN crystal growth

The simulation was performed after constructing the thermal field and setting the necessary parameters such as the thermal conductivity and emissivity for each kind of material, the crystal density and the wetting angle. The software was operated using iterative method according to the divisiory grids. The melt flow and airflow were first adjusted on the basis of an initial status. The simulation will come into the next stage if the convergence criterion is satisfactory, which means that a stable status was obtained. Then the interface will be adjusted until the stable melt convection was acquired finally. The model in this software deals with the symmetrical system in cylinder shape, which is not suitable for the non-cylindrical one. In our crystal growth system, a Pt crucible was placed on several pieces of ZrO_2 plates in the center of an alumina crucible. There is a cone-shaped corundom shield and a cylindrical alumina cap with an alumina tube covered on the Pt crucible for better insulation. Three kinds of thermal system A, B and C were simulated for comparison. A is the hanging crucible system with an inner Pt sleeve in the height of 40 mm. B is the hanging crucible system with a 70 mm inner Pt sleeve in height. C is the traditional Czochralski system. The main parameters used in the numerical simulation are listed in Table S1. In our simulation, the interface shape is flat under a rotation of 3 rpm and a pulling rate of 0.4 mm/h for system A, 3 rpm and 0.5 mm/h for system B, and 2 rpm and 0.4 mm/h for system C, respectively. It should be noted that the flow in system C is not stable at 2 rpm and 0.4 mm/h, even the rotation speed and pulling rate are regulated drastically. This may be induced by the much too strong natural convection in our present thermal field configuration. So we choose the same rotation speed of 3 rpm and pulling rate of 0.4 mm/h for comparison in our numerical simulation. The heating power was maintained at a constant of 1.6 kW, due to the little influence of change in heating power on the simulation and the fact that the power remains nearly the same during the crystal growth process. The simulated results of the thermal and flow fields, the isothermal curve and the thermal stress distribution are shown in Fig. S3.

Table S1 Main parameters used in numerical simulation.

Property	Value
Density of the crystal (g/cm^3)	4.63
Emissivity of the crystal	0.3
Specific heat of the crystal (J/gK)	0.62
Thermal conductivity of the crystal (W/mK)	6.9
Density of the melt (g/cm^3)	3.67
Emissivity of the melt	0.3
Specific heat of the melt (J/gK)	800
Thermal conductivity of the melt (W/mK)	5.0
Emissivity of the Pt crucible	0.9
Specific heat of the Pt crucible (J/gK)	0.13
Thermal conductivity of the Pt crucible (W/mK)	71.6
Electricity conductivity of the Pt crucible (S/m)	9.4×10^6
Emissivity of alumina	0.4
Thermal conductivity of alumina (W/mK)	2.15
Emissivity of ZrO_2	0.6
Thermal conductivity of ZrO_2 (W/mK)	2.14

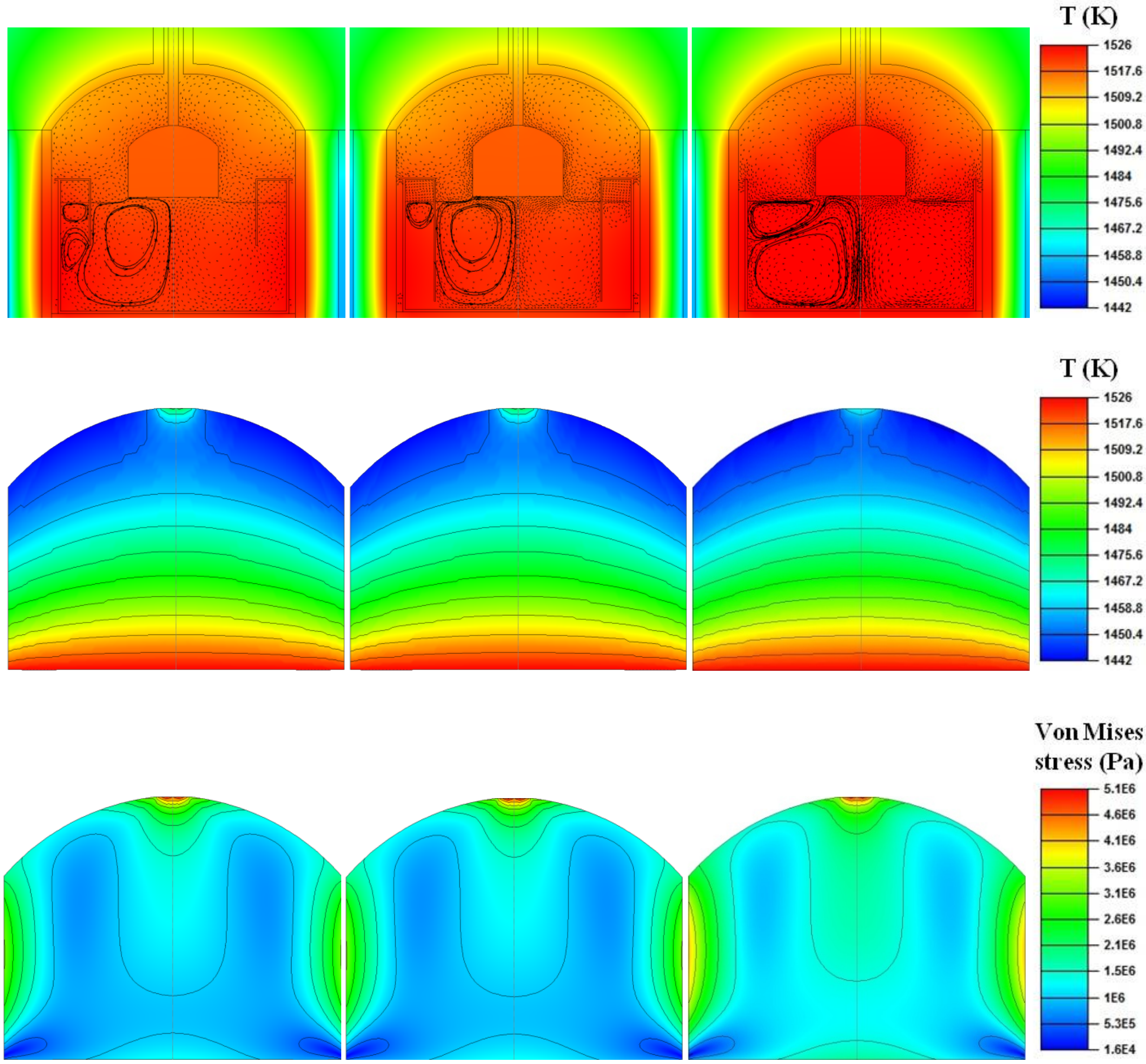

A B C

Fig. S3 The thermal and flow fields (upper), the isothermal curve (middle) and the thermal stress distribution (lower) of three different thermal systems A, B and C. A is the hanging crucible system with an inner Pt sleeve in the height of 40 mm, B is that with a 70 mm inner Pt sleeve in height, and C is the traditional Czochralski system.

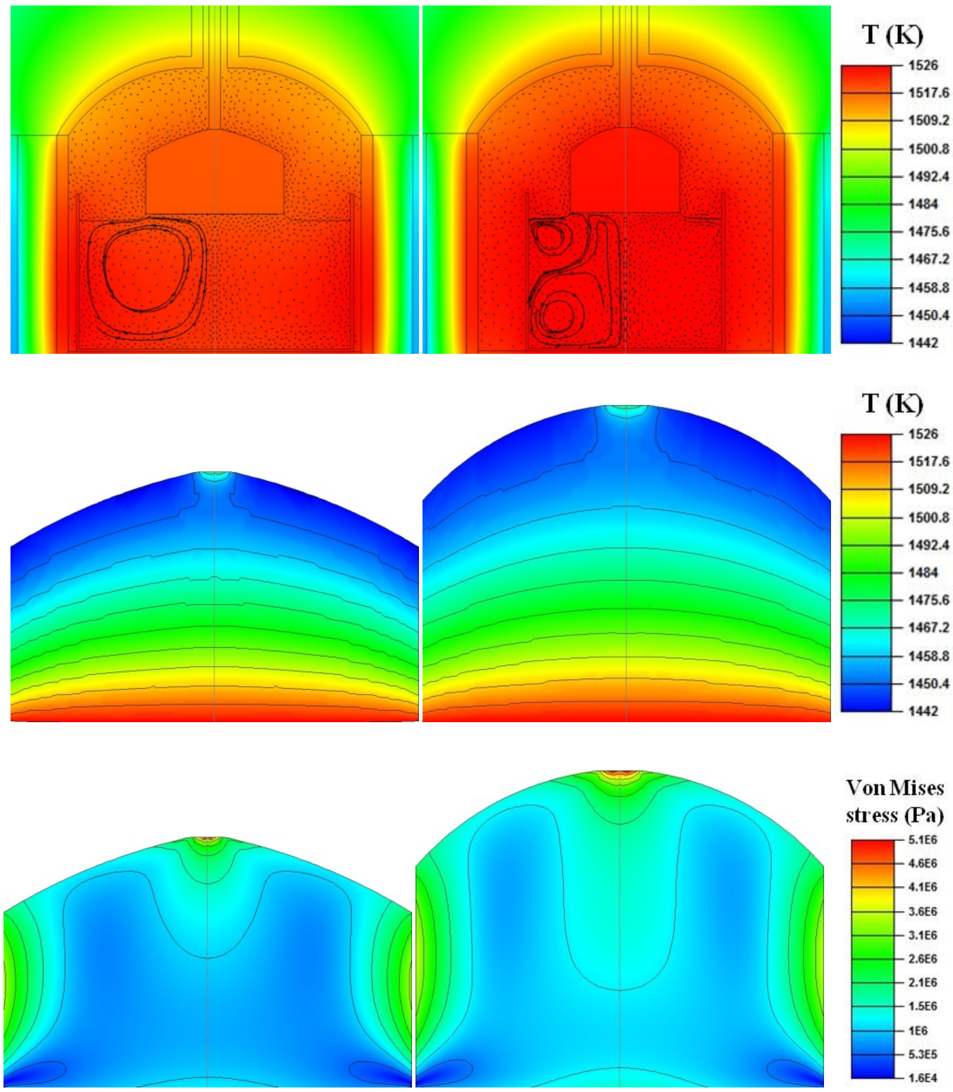

(a) (b)

Fig. S4 The thermal and flow fields (upper), the isothermal curve (middle) and the thermal stress distribution (lower) of the traditional CZ system with (a) a crystal of 70 mm in diameter in a 140 mm crucible and (b) a crystal of 55 mm in diameter in a 100 mm crucible.

Crystallinity of SLN and MgOSLN crystals

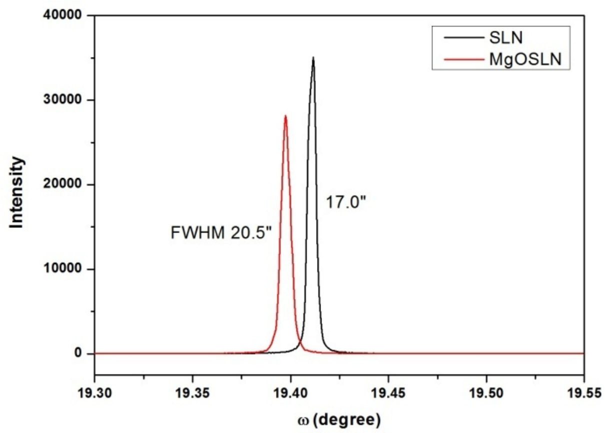

Fig. S5 Rocking curve of SLN and MgOSLN crystals.

Optical homogeneity of MgOSLN sample

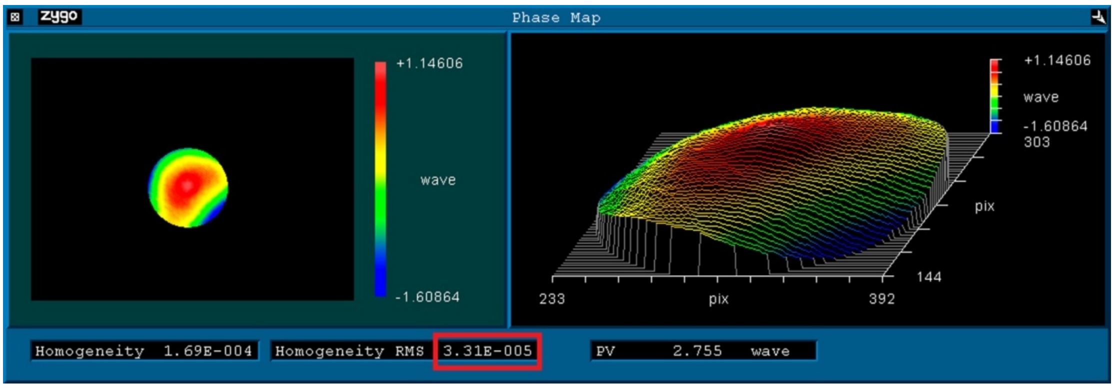

Fig. S6 Optical homogeneity of MgOSLN crystal.

Variation of density at different temperatures

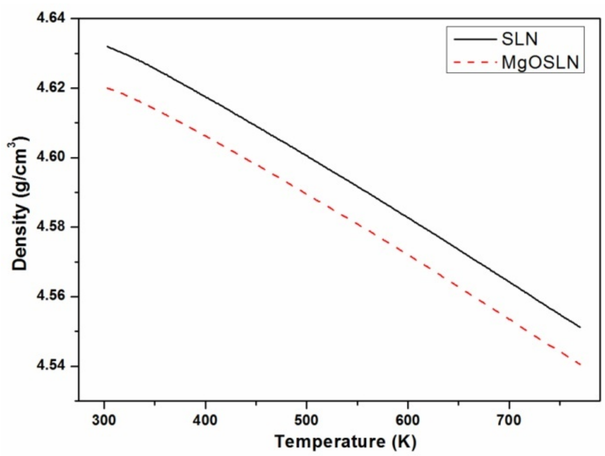

Fig. S7 Density curves vs temperature of SLN and MgOSLN crystals.